Korean Journal of Radiology

KJR

Check for updates

Right Ventricular Mass Quantification Using Cardiac CT and a Semiautomatic Three-Dimensional Hybrid Segmentation Approach: A Pilot Study

Hyun Woo Goo

Department of Radiology and Research Institute of Radiology, University of Ulsan College of Medicine, Asan Medical Center, Seoul, Korea

Objective: To evaluate the technical applicability of a semiautomatic three-dimensional (3D) hybrid CT segmentation method for the quantification of right ventricular mass in patients with cardiovascular disease.
Materials and Methods: Cardiac CT (270 cardiac phases) was used to quantify right ventricular mass using a semiautomatic 3D hybrid segmentation method in 195 patients with cardiovascular disease. Data from 270 cardiac phases were divided into subgroups based on the extent of the segmentation error (no error; ≤ 10% error; > 10% error [technical failure]), defined as discontinuous areas in the right ventricular myocardium. The reproducibility of the right ventricular mass quantification was assessed. In patients with no error or < 10% error, the right ventricular mass was compared and correlated between paired end-systolic and end-diastolic data. The error rate and right ventricular mass were compared based on right ventricular hypertrophy groups.
Results: The quantification of right ventricular mass was technically applicable in 96.3% (260/270) of CT data, with no error in 54.4% (147/270) and ≤ 10% error in 41.9% (113/270) of cases. Technical failure was observed in 3.7% (10/270) of cases. The reproducibility of the quantification was high (intraclass correlation coefficient = 0.999, $p < 0.001$). The indexed mass was significantly greater at end-systole than at end-diastole (45.9 ± 22.1 g/m^2 vs. 39.7 ± 20.2 g/m^2, $p < 0.001$), and paired values were highly correlated ($r = 0.96$, $p < 0.001$). Fewer errors were observed in severe right ventricular hypertrophy and at the end-systolic phase. The indexed right ventricular mass was significantly higher in severe right ventricular hypertrophy ($p < 0.02$), except in the comparison of the end-diastolic data between no hypertrophy and mild hypertrophy groups ($p > 0.1$).
Conclusion: CT quantification of right ventricular mass using a semiautomatic 3D hybrid segmentation is technically applicable with high reproducibility in most patients with cardiovascular disease.
Keywords: *Cardiac CT; Cardiovascular disease, Right ventricular hypertrophy; Right ventricular mass; Threshold-based segmentation*

INTRODUCTION

Right ventricular mass as a quantitative measure of right ventricular hypertrophy is one of the key prognostic

parameters in cardiovascular disease [1-3]. Due to the inaccuracy in echocardiographic measurements of the right ventricular mass, accurate and reproducible quantification has been typically performed using cardiac MRI [3-8] with cardiac CT demonstrating comparable results [9-12]. When quantifying right ventricular mass using CT or MRI, the papillary muscles and trabeculations can either be excluded from [6-11] or included in [7-9] the myocardial mass. The previous studies showed that their inclusion increases right ventricular mass by 79% in patients with repaired tetralogy of Fallot [7], and contributes to a 35% increase in the total right ventricular mass in patients with pulmonary arterial hypertension [8]. Consequently, the papillary muscles and trabeculations should not be neglected when quantifying

right ventricular mass. However, manual segmentation of heavy trabeculations in the right ventricle is time-consuming and decreases reproducibility. A hybrid segmentation technique using advanced thresholding and region-growing can overcome the limitations of manual segmentation [7,9]. Recently, we reported that semiautomatic three-dimensional (3D) hybrid segmentation could successfully quantify left ventricular mass [13]. However, its technical applicability in quantifying right ventricular mass remains to be determined, as the right ventricular wall is thinner, particularly in the apical portion, and more heavily trabeculated. Therefore, this study evaluated the technical applicability of a semiautomatic 3D hybrid CT segmentation method for the quantification of right ventricular mass in patients with cardiovascular disease.

MATERIALS AND METHODS

This retrospective study was approved by the local Institutional Review Board and the requirement for informed consent was waived (IRB No. 2020-0931).

Study Population

A total of 195 consecutive patients (median age 13.0 months, range 1 day–60 years; M:F = 110:85; median body surface area 0.4 m^2, range 0.2–2.1 m^2) who underwent cardiac CT examination between September 2013 and December 2016 using a dual-source scanner (SOMATOM Definition Flash; Siemens Healthineers) for morphologic and functional assessments of the cardiovascular system including right ventricular mass quantification were enrolled in this study. Exclusion criteria included poor contrast enhancement or severe artifacts in the right ventricle and a rudimentary or non-visible right ventricle. The study population had various cardiovascular diseases (Table 1).

Cardiac CT

Cardiac CT scan parameters were as follows: 2 x 64 x 0.6-mm slices with the z-flying focal spot technique, 0.28 second gantry rotation time, 75 ms temporal resolution, 0.75 mm slice width, and 0.4 mm reconstruction interval. The cardiac CT scan range included the whole thorax in all patients, except three (Kawasaki disease, 2; hypertrophic cardiomyopathy, 1) in whom the whole heart was covered. A combined tube current modulation (CARE Dose 4D; Siemens Healthineers) was used in all CT scans. Free-breathing prospectively electrocardiography (ECG)-triggered sequential

Table 1. Cardiovascular Abnormalities of Study Population

Cardiovascular Abnormality	Number of Patients
Tetralogy of Fallot	47
Pulmonary atresia with ventricular septal defect	20
Coarctation of the aorta	17
Double outlet right ventricle	14
Functional single ventricle	14
Complete transposition of the great arteries	13
Congenitally-corrected transposition of the great arteries	11
Ventricular septal defect	9
Atrial septal defect	7
Pulmonary atresia with intact ventricular septum	7
William syndrome	5
Interrupted aortic arch	4
Critical aortic stenosis	4
Truncus arteriosus	3
Total anomalous pulmonary venous return	3
Double aortic arch	3
Ebstein anomaly	2
Kawasaki disease	2
Bicuspid aortic valve	2
Absent pulmonary valve syndrome	1
Left pulmonary artery sling	1
Coronary artery fistula	1
Congenital aortic regurgitation	1
Critical pulmonary stenosis	1
Status post heart transplantation	1
Hypertrophic cardiomyopathy	1
Pulmonary arteriovenous fistula	1
Total	195

scan was used in 66.2% (129/195) of patients (mean age 12.8 ± 26.1 months) and breath-hold retrospectively ECG-gated spiral scan was used in 33.8% (66/195) of patients (mean age 19.7 ± 10.9 years). For free-breathing CT examination, 129 children, usually younger than 6 years of age, were initially sedated with oral chloral hydrate (50 mg/kg) and subsequently with intravenous midazolam (0.1 mg/kg) or ketamine (1 mg/kg) as required. Of the 129 children, prospective ECG triggering was used in 47 children (mean age 2.2 ± 3.3 months). Respiratory triggering using a respiratory gating system (AZ-733V; Anzai Medical Co.), as previously described [14,15], was added to the ECG-triggered sequential scanning in the remaining 82 children (mean age 19.1 ± 31.3 months). A total of 270 cardiac phases were obtained in 195 patients: 191 end-systolic phases and 79 end-diastolic phases; 75 paired end-systolic and end-diastolic phases in the same patients. The mean

heart rate was 108.6 ± 26.2 beats per minute (bpm) (range 53.0–168.5) during the end-systolic acquisitions and 96.3 ± 27.1 bpm (range 52.0–158.0) during the end-diastolic acquisitions.

To reduce CT radiation dose, body size-adapted dose protocols were used [16,17]. To further reduce the CT radiation dose of retrospectively ECG-gated spiral scans, ECG-controlled tube current modulation (MinDose; Siemens Healthineers) and biphasic chest pain protocol, in which the tube current outside the heart is reduced to half by turning off one of two X-ray tubes in a dual-source scanner, were utilized [16]. To maximize radiation dose efficiency and iodine contrast-to-noise ratio, the lowest possible tube voltage preventing substantial tube current saturation and thus resultant degradation of image quality was selected: 70 kV (n = 120, 61.5%), 80 kV (n = 23, 11.8%), 100 kV (n = 51, 26.2%), and 120 kV (n = 1, 0.5%). The mean volume CT dose index and dose-length product values based on a 32-cm phantom were 5.5 ± 5.9 mGy and 170.8 ± 258.8 mGy·cm, respectively. The mean effective dose estimate of cardiac CT calculated by multiplying the dose-length product and the age, gender, and tube voltage-specific conversion factors for chest CT [18] was 2.6 ± 3.1 mSv. These three CT radiation dose metrics varied depending on the CT scan mode, patient size, and the number of cardiac phases obtained during the CT examination (Table 2).

Homogeneous opacification of the right and left sides of the ventricles is of critical importance in applying a threshold-based segmentation approach for ventricular volumetry. Briefly, to achieve this goal, a multi-phase injection protocol using a diluted contrast agent and decremental injection rates is the key to allow overlapping of prolonged ventricular peak enhancement on both sides. The iodinated contrast agent (Iomeron 400, iomeprol 400 mgI/mL; Bracco Imaging SpA; 1.5–2.0 mL/kg) was administered intravenously with a dual-head power injector

at an injection rate of 0.3–3.0 mL/s depending on the sizes of the patient's body and angiocatheter. A larger amount (2.0 mL/kg) was necessary for selected cases with a large intracardiac or extracardiac shunt, substantial valvular regurgitation, a severely enlarged heart, and severely impaired cardiac function, as described previously [19]. A tri-phasic or quadri-phasic injection protocol was utilized to achieve uniform cardiovascular enhancement and minimal peri-venous streak artifacts from the undiluted contrast agent [15]. The scan delay time was determined by a bolus tracking technique.

Quantification of Right Ventricular Mass and Volume

Each patient's thin axial cardiac CT dataset was evaluated using a commercially available workstation (Advantage Windows 4.6; GE Healthcare). To quantify right ventricular volume and mass, a previously reported semiautomatic 3D threshold-based segmentation method, in which the papillary muscles and trabeculations are excluded from the ventricular cavity and included in the ventricular myocardium, was used [13]. As previously described for the quantification of left ventricular mass [13], the epicardial border of the right ventricle was outlined serially using the one-click identification of the right ventricle as commonly used in the automatic identification of coronary arteries, 3D region-growing method, and manual adjustment. The right ventricular cavity volume was obtained by applying a threshold to the total right ventricular volume. A threshold to separate the most compact interventricular septal myocardium from adjacent ventricular blood for each cardiac phase was determined using a histogram-assisted analysis (Fig. 1) [20]. Therefore, unlike the interventricular septal myocardium, some of the trabeculated endocardial myocardium along the right ventricular free wall might be included in the ventricular cavity due to the partial volume effect. This strategy was used to improve consistency in

Table 2. CT Radiation Dose Parameters according to Cardiac CT Scan Modes

CT Scan Mode	Volume CT Dose Index (mGy)	Dose-Length Product (mGy·cm)	Effective Dose (mSv)
Prospectively ECG-triggered sequential scan			
Total (n = 130)	1.7 ± 1.6	19.0 ± 21.9	0.9 ± 0.7
One (ES or ED) cardiac phase (n = 92)	1.1 ± 0.4	11.3 ± 6.8	0.6 ± 0.2
Two (ES and ED) cardiac phases (n = 38)	3.2 ± 2.3	38.4 ± 32.6	1.7 ± 0.7
Retrospectively ECG-gated spiral scan			
Total (n = 65)	13.0 ± 3.8	474.2 ± 248.6	6.1 ± 3.1
One (ES or ED) cardiac phase (n = 23)	12.1 ± 3.8	260.3 ± 97.6	3.6 ± 1.5
Two (ES and ED) cardiac phases (n = 42)	13.6 ± 3.5	591.4 ± 227.2	7.4 ± 2.9

ECG = electrocardiography, ED = end-diastolic, ES = end-systolic
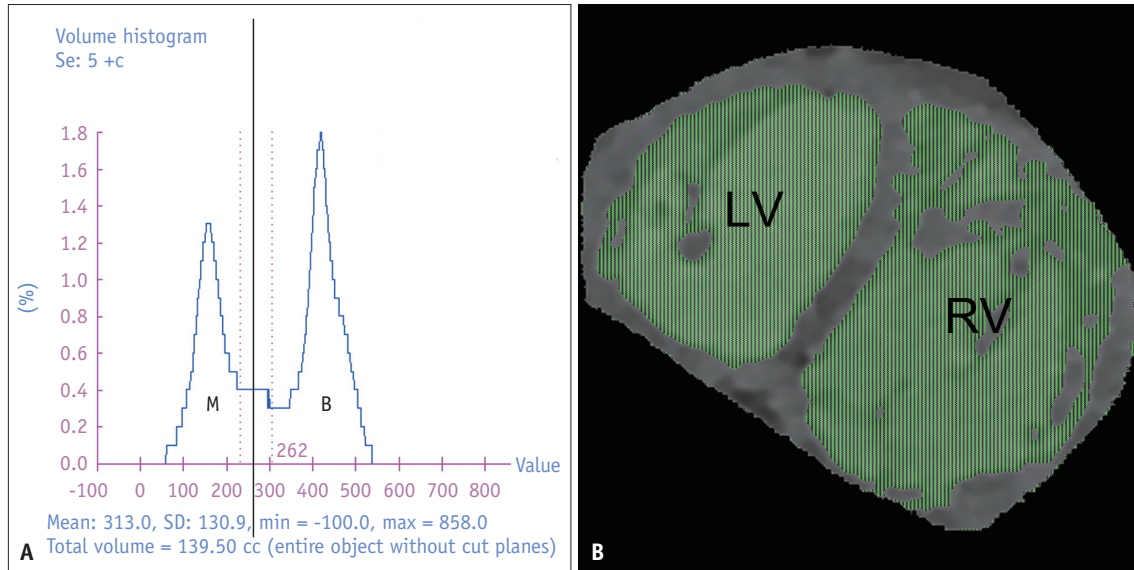
Fig. 1. An 8-month-old boy with congenitally-corrected transposition of the great arteries who underwent pulmonary artery banding, demonstrating a histogram-assisted determination of an optimal threshold.
A. Histogram shows that the threshold (black vertical line) used for segmentation is more closely located to the distribution of the ventricular M than to that of the ventricular B in order to exclude voxels consisting of 100% ventricular M consistently. **B.** End-diastolic four-chamber cardiac CT image reveals the segmented ventricular B in green. Notably, unlike the interventricular septal M, some of the trabeculated endocardial M along the right ventricular free wall are included in the ventricular B due to the partial volume effect. B = blood, LV = left ventricle, M = myocardium, RV = right ventricle

determining a threshold by avoiding visual perception errors. Right ventricular mass was calculated by subtracting the ventricular cavity volume from the total ventricular volume for each cardiac phase. This value was multiplied by the specific gravity of the myocardium (1.05 g/mL). All volumetric measurements were indexed to the patient's body surface area recorded at the cardiac CT examination.

Volumetric segmentation was conducted by a radiology technologist (11 years of experience in cardiac CT image processing) and validated by a radiologist (21 years of experience in cardiac CT). The right ventricular mass-volume ratio was calculated for each cardiac phase. To assess this method's technical applicability for right ventricular mass quantification, data were divided qualitatively into subgroups based on the extent of segmentation errors (i.e., any discontinuous areas in the right ventricular myocardium identified on axial, coronal, and sagittal reformatted images and volume-rendered image with 100% opacity of the segmented right ventricular myocardium): subgroup 1 (no error) (Figs. 2, 3 [end-systolic phase]), subgroup 2 (trivial error) (Fig. 3 [end-diastolic phase], Fig. 4), and subgroup 3 (extensive error; it was defined as technical failure) (Fig. 5).

Reproducibility of Right Ventricular Mass Measurements

Right ventricular mass in a subset of randomly selected

20 cardiac phases from 20 patients, consisting of 10 patients without hypertrophy and 10 patients with hypertrophy, were quantified twice. Inter-measurement variability was represented as the mean difference (%) and the intraclass correlation coefficient (ICC) between the two measurements.

Right Ventricular Hypertrophy

Since a quantitative diagnostic criterion of right ventricular hypertrophy was not available for the segmentation method used in this study, the degree of right ventricular hypertrophy was assessed visually on cardiac CT and was categorized into no hypertrophy, mild hypertrophy (i.e., less extensive), and severe hypertrophy (i.e., more extensive). The absence of right ventricular hypertrophy was based on the clinical experience of cardiothoracic CT imaging in patients with a normal-looking right ventricle. Nevertheless, accurate differentiation of no hypertrophy from mild hypertrophy was difficult, which exactly reflects a pitfall commonly experienced in our clinical practice. Hypertrophy was determined based on whether the right ventricular free wall was thinner (mild hypertrophy) or thicker (severe hypertrophy) than the left ventricular wall. Right ventricular free wall thickness including the myocardial compact layer only and excluding the
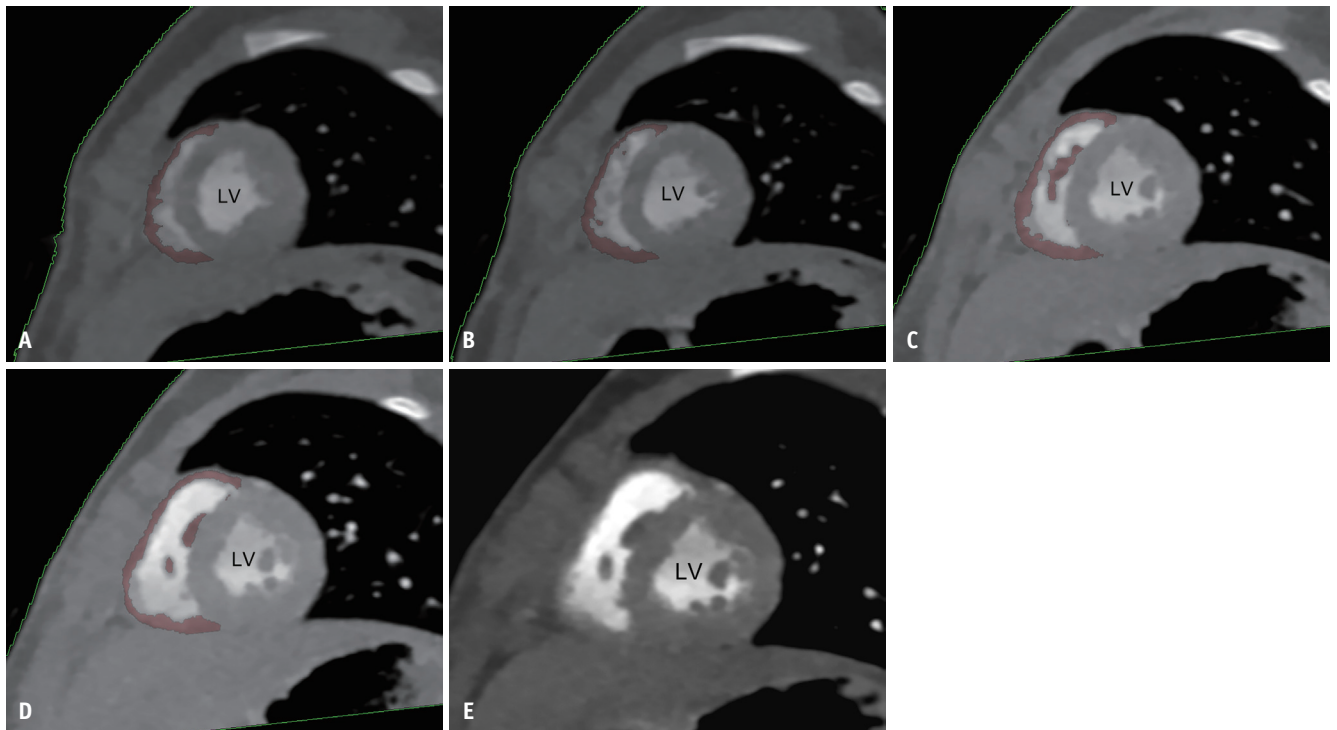
Fig. 2. A 13-month-old boy with repaired coarctation of the aorta, showing no segmentation errors.
A-D. End-systolic short-axis cardiac CT images show the segmented right ventricular free wall in pink without any segmentation errors. **E.** End-systolic short-axis cardiac CT image without color overlay matched with figure two-dimensional for head-to-head comparison. LV = left ventricle

trabeculations was measured at the mid-ventricular level on the axial cardiac CT image and indexed to the patient's body surface area.

Statistical Analysis

Continuous variables are presented as mean ± standard deviation or median with range, and categorical variables are expressed as a frequency with percentage. Paired t tests compared means of paired continuous variables. Pearson correlation coefficients analyzed the degree of correlation between paired continuous variables. Between group comparisons of continuous variables were analyzed using unpaired t test. A chi-square test analyzed the association between two categorical variables. An ICC evaluated the reproducibility of right ventricular mass measurements. A p value of less than 0.05 was considered statistically significant. Statistical analyses were performed using statistical software (SPSS version 24.0; IBM Corp.).

RESULTS

Technical Applicability

Right ventricular mass quantification was technically applicable in 96.3% (260/270) of CT data, consisting of

subgroup 1 (no error) in 54.4% and subgroup 2 (trivial error) in 41.9%. Errors were most commonly located at the apical portion (Figs. 3, 4). Technical failure was observed in 3.7% (10/270) of cases.

Quantification of Right Ventricular Mass

In 69 patients who had both end-systolic and end-diastolic data after excluding 6 pairs demonstrating extensive segmentation errors, the indexed mass was significantly higher at end-systole than at end-diastole (45.9 ± 22.1 g/m^2 vs. 39.7 ± 20.2 g/m^2, $p < 0.001$) and the paired values demonstrated a high correlation ($r = 0.96$, $p < 0.001$) (Fig. 6). In the subset of 20 patients assessed for reproducibility, the two right ventricular mass measurements were 16.3 ± 14.8 g and 16.9 ± 15.2 g, respectively, with a mean difference of $5.5 \pm 3.4\%$ and were highly reproducible (ICC = 0.999, 95% confidence interval, 0.995–1.000; $p < 0.001$).

Right Ventricular Hypertrophy

Fewer errors were seen in the more severe right ventricular hypertrophy group and in the end-systolic data. (Table 3, all p values < 0.001) (Fig. 3).

Pearson correlation coefficients between the indexed
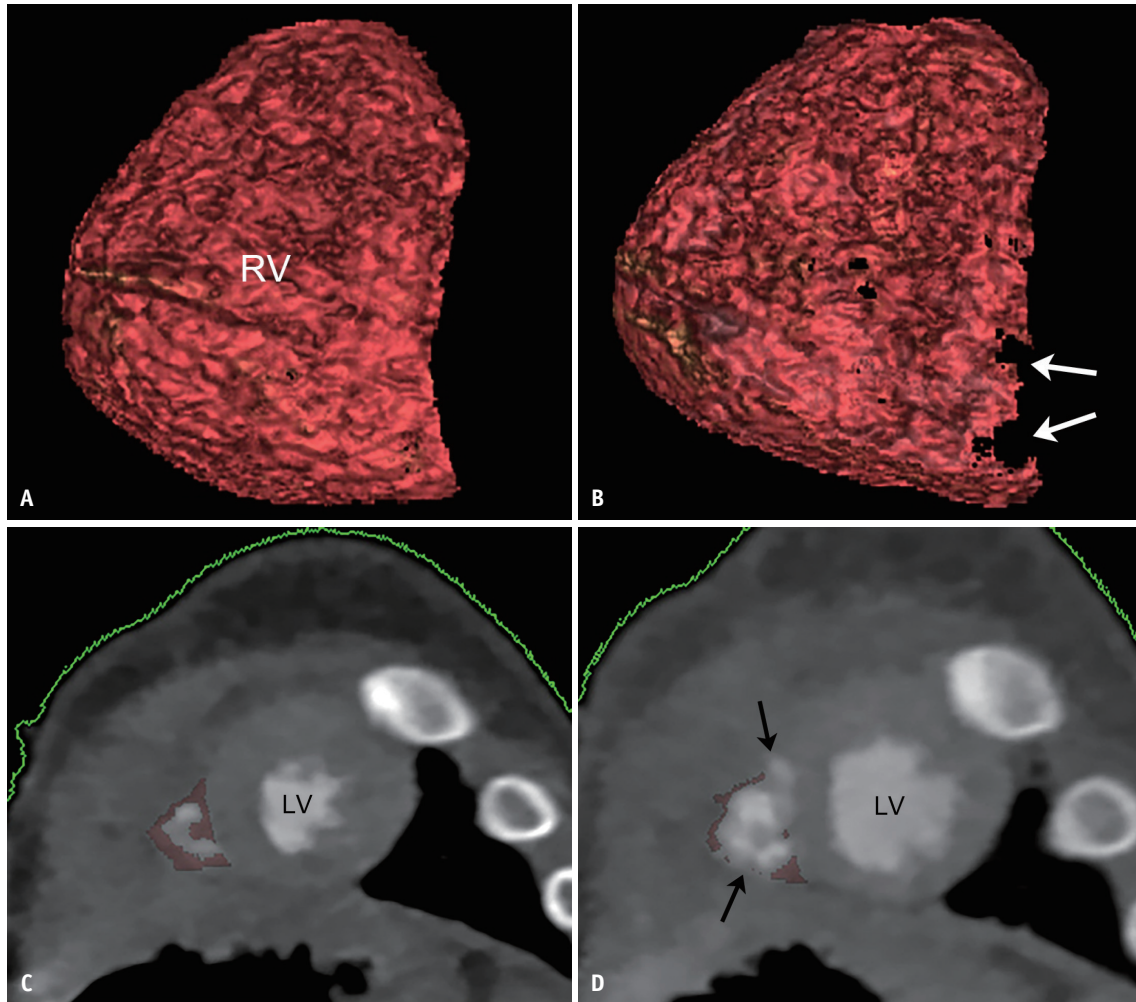
Fig. 3. A 7-month-old girl with repaired coarctation of the aorta, showing no errors at the end-systolic phase and trivial errors at the end-diastolic phase.
A-D. End-systolic volume-rendered **(A)** and short-axis **(C)** cardiac CT images show the segmented right ventricular free wall in pink without any segmentation errors in the right ventricular mass quantification. In contrast, small areas of segmentation errors (arrows) are shown on the end-diastolic volume-rendered **(B)** and short-axis **(D)** cardiac CT images. LV = left ventricle, RV = right ventricle

masses and the indexed wall thickness were weak (end-systolic phase: $r = 0.35$, $p < 0.004$; end-diastolic phase: $r = 0.27$, $p < 0.03$).

The indexed right ventricular mass at the end-systolic phase was greater than that at the end-diastolic phase in all patients with or without right ventricular hypertrophy, but the difference was greater with increased right ventricular hypertrophy (7.1% for no hypertrophy, 14.3% for mild hypertrophy, and 14.9% for severe hypertrophy) (Table 4). Moreover, the indexed right ventricular mass and wall thickness as well as the right ventricular mass-volume ratio tended to be greater with increased hypertrophy for each cardiac phase (Table 4).

DISCUSSION

This study demonstrated the technical applicability of a semiautomatic 3D hybrid CT segmentation method for quantifying right ventricular mass in the majority of cases (95.4% [186/195] of patients, 96.3% [260/270] of cardiac phases), demonstrating no or trivial segmentation error. However, this hybrid approach was not perfect in nearly half of the cases. The main cause of segmentation error was the thin right ventricular wall, most commonly at the apical portion. Fewer errors were observed in cases with more severe hypertrophy and at the end-systolic phase, and the right ventricular free wall is thicker in these two conditions. These errors could be corrected with a computer-aided design, where the right ventricular wall is artificially
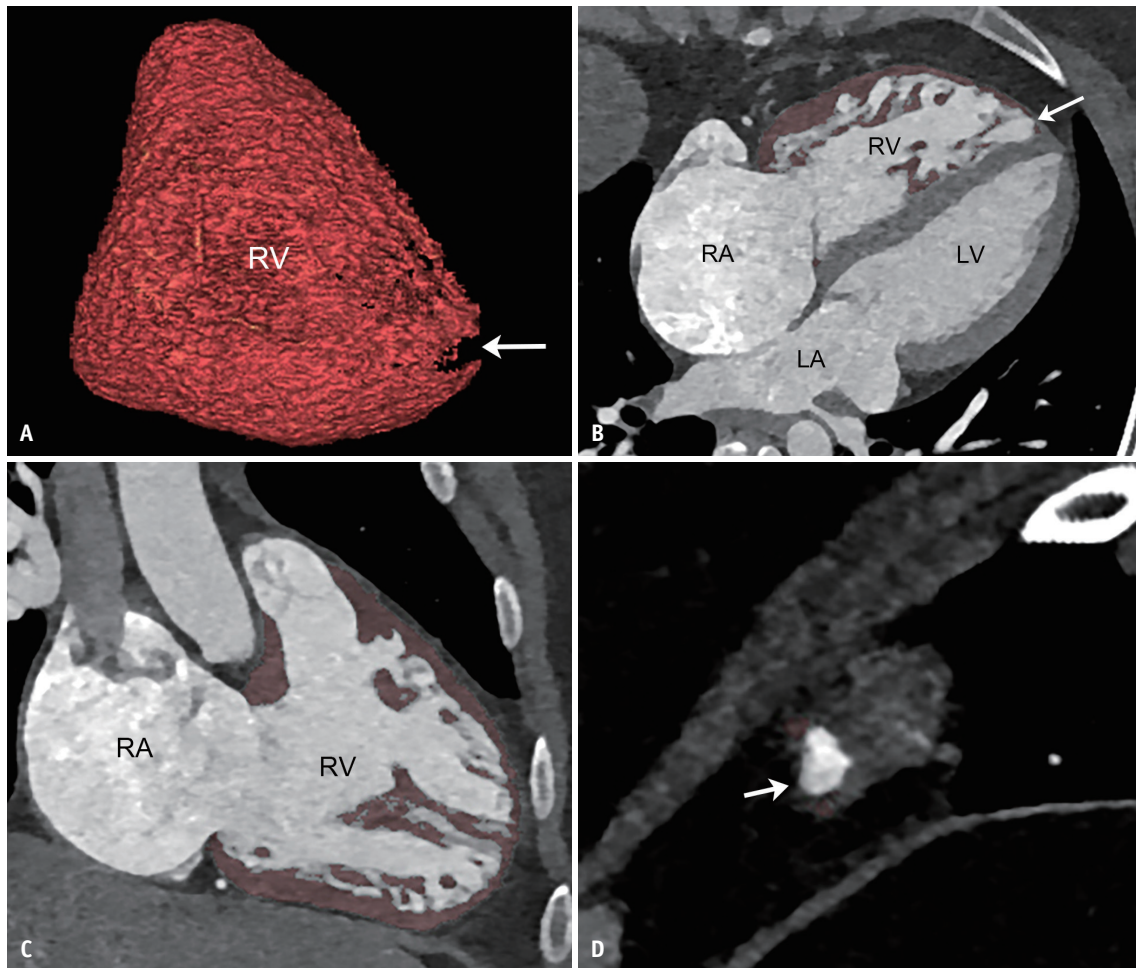
Fig. 4. A 32-year-old woman with atrial septal defect, showing trivial segmentation errors.
A-D. End-diastolic volume-rendered **(A)**, long-axis **(B, C)**, and short-axis **(D)** cardiac CT images reveal small areas of segmentation errors (arrows) in the right ventricular mass quantification. LA = left atrium, LV = left ventricle, RA = right atrium, RV = right ventricle
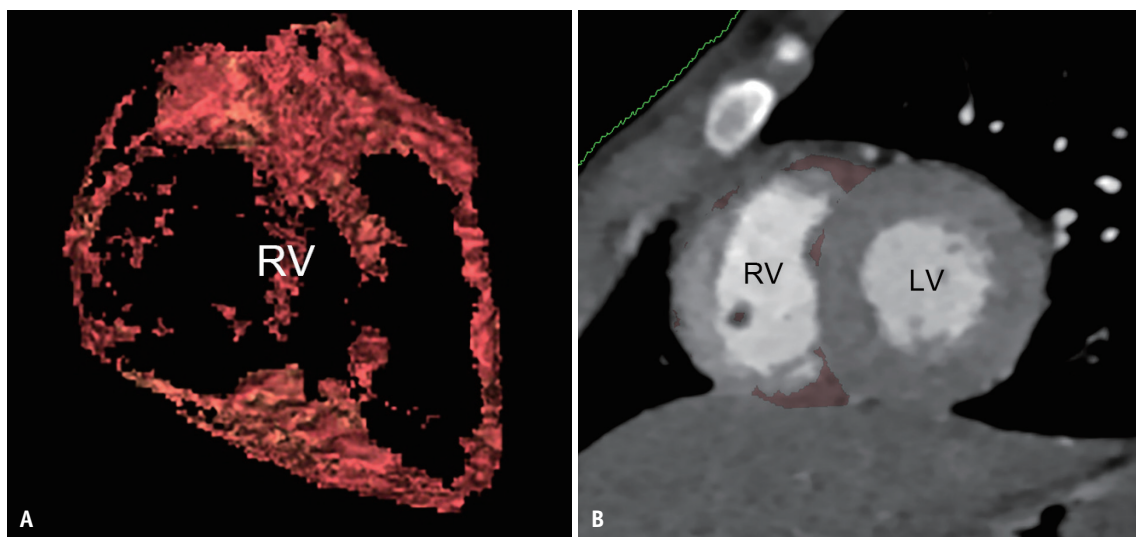
Fig. 5. A 13-month-old boy with repaired complete transposition of the great arteries, showing extensive segmentation errors.
A, B. End-systolic volume-rendered **(A)** and short-axis **(B)** cardiac CT images demonstrate extensive areas of segmentation errors in the right ventricular mass quantification owing to the thin right ventricular free wall. LV = left ventricle, RV = right ventricle

designed with a minimum thickness (e.g., < 1.0 mm) and added to the segmented right ventricular mass, which is commonly known for producing a virtual 3D model [21].

Theoretically, the myocardial mass should remain the same, regardless of the cardiac phase. Using the same CT segmentation, a previous study demonstrated that the indexed end-systolic left ventricular mass was 7.7% greater
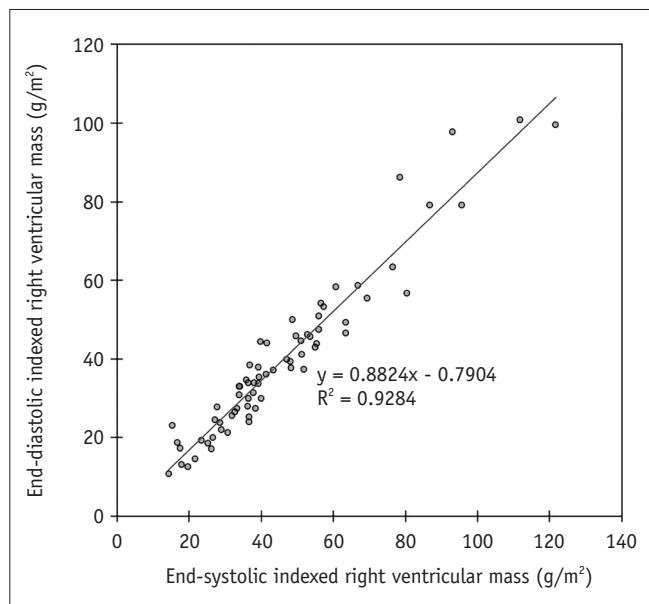
Fig. 6. Scatter plot between indexed end-systolic and end-diastolic right ventricular mass values obtained from 69 patients with paired end-systolic and end-diastolic phases. Pearson correlation coefficient of the scatter plot was 0.96, indicating a high positive linear correlation between the paired indexed right ventricular mass values obtained at the end-systolic and end-diastolic phases. Retrospectively ECG-gated spiral scan was performed in 35 patients and prospectively ECG-triggered sequential scan was obtained in 34 patients. ECG = electrocardiography

than the indexed end-diastolic mass, and a very high correlation ($r = 0.99$) was found between the end-systolic and end-diastolic phases [13]. Similarly, the indexed end-systolic right ventricular mass in this study was also significantly greater than the indexed end-diastolic mass, and the difference (13.5%) was slightly larger than that in the left ventricle. The Pearson correlation coefficient ($r = 0.96$) for right ventricular mass (end-systolic vs. end-diastolic) was slightly lower than that for left ventricular mass ($r = 0.99$) [13] and was similar to that for right ventricular mass ($r = 0.97$) previously reported [3]. These differences could be attributed to a greater partial volume effect in the right ventricle due to heavy trabeculations, where more voxels containing both blood and myocardium along the endocardial border may be included in the ventricular cavity (i.e., partial volume effect). While the right ventricular mass is typically calculated at end-diastole [7,10], based on the results of this study, it is worthwhile to consider the quantification of end-systolic, rather than end-diastolic, right ventricular mass as a clinical standard.

Evidence suggests that right ventricular mass quantified using simplified contouring, in which the papillary muscles and trabeculations are excluded from the myocardial volume, is considerably underestimated. Compared to a simplified contouring method, the threshold-based segmentation method includes the papillary muscles and trabeculations into the myocardial volume and has the potential to provide a more accurate and reproducible right ventricular mass [7]. In patients with repaired tetralogy of Fallot, the end-diastolic right ventricular mass quantified using a semiautomatic threshold-based segmentation was 79%

Table 3. Frequency of Segmentation Error in Three RVH Groups (Total 270 Cardiac Phases)

Segmentation Error	No RVH		Mild RVH		Severe RVH	
	ES (n = 49, %)	ED (n = 17, %)	ES (n = 106, %)	ED (n = 53, %)	ES (n = 36, %)	ED (n = 9, %)
Subgroup 1 (no error)	20 (40.8)	4 (23.5)	75 (70.8)	10 (18.9)	34 (94.4)	4 (40.0)
Subgroup 2 (trivial error)	26 (53.1)	10 (58.8)	31 (29.2)	39 (73.6)	2 (5.6)	5 (60.0)
Subgroup 3 (extensive error)	3 (6.1)	3 (17.6)	0 (0.0)	4 (7.5)	0 (0.0)	0 (0.0)

ED = end-diastolic, ES = end-systolic, RVH = right ventricular hypertrophy

Table 4. Right Ventricular Measures in Three RVH Groups (69 Patients with Paired ES and ED Phases)

Right Ventricular Measures	No RVH (n = 13)		Mild RVH (n = 47)		Severe RVH (n = 9)	
	ES	ED	ES	ED	ES	ED
Indexed mass (g/m²)	33.7 ± 19.5	31.3 ± 21.3	44.9 ± 19.6	38.5 ± 18.2	68.5 ± 23.2	58.3 ± 19.5
Indexed wall thickness (mm/m²)	3.2 ± 1.8	2.0 ± 1.0	10.7 ± 8.8	5.4 ± 4.4	26.7 ± 13.8	13.7 ± 9.5
Indexed volume (mL/m²)	61.4 ± 30.9	118.5 ± 51.2	47.8 ± 28.4	109.1 ± 49.1	33.9 ± 24.8	88.0 ± 41.8
Mass-volume ratio (g/mL)	0.7 ± 0.5	0.3 ± 0.3	1.3 ± 0.7	0.4 ± 0.2	2.8 ± 1.6	0.8 ± 0.3

ED = end-diastolic, ES = end-systolic, RVH = right ventricular hypertrophy

greater than that quantified using simplified contouring [7]. Furthermore, the papillary muscles and trabeculations showed a large contribution to the total right ventricular mass in both patients with pulmonary arterial hypertension (35%) and controls (25%) [8].

The segmentation method used in this study demonstrated an excellent reproducibility (mean difference, $5.5 \pm 3.4\%$; ICC, 0.999) between two right ventricular mass measurements. This is slightly greater than that ($2.3 \pm 1.1\%$) of left ventricular mass in a previous study [13], reflecting the more complicated and diverse right ventricular geometry. Additionally, less processing time is required for the threshold-based method (67 seconds) [7], compared with manual tracing of the right ventricular papillary muscles and trabeculations (21 minutes) [8]. Unfortunately, the processing time for the quantification of the right ventricular mass was not recorded in this study. Because studies on automated calculation of ventricular mass using deep learning are currently active [22], the processing time will become shorter in the near future.

Normal right ventricular mass in children and young adults measured using cardiac MRI have been reported [6,23,24]; however, only one used a semiautomatic threshold-based analysis, reporting 17.6 g/m^2 for females and 20.5 g/m^2 for males [24]. Additionally, the indexed right ventricular mass that included the papillary muscles and trabeculations was 19.0 g/m^2 in 20 control subjects without no pulmonary and cardiovascular disease [8]. The indexed right ventricular mass without hypertrophy in this study was slightly higher (31.3–33.7 g/m^2) than the previously reported normal values. On the other hand, the indexed right ventricular mass that included the papillary muscles and trabeculations was 51.0 g/m^2 in patients with repaired tetralogy of Fallot [7] and 49.0–50.0 g/m^2 in patients with pulmonary arterial hypertension [8]. These published values are approximately in the middle between mild (38.5–44.9 g/m^2) and severe hypertrophy (58.3–68.5 g/m^2) in this study.

In this study, the right ventricular mass-volume ratios were higher in the more severe hypertrophy group. In patients with repaired tetralogy of Fallot, high right ventricular mass-volume ratio demonstrated a strong association with subsequent increase in right ventricular end-diastolic volume [3], a preoperative predictor of death and sustained ventricular tachycardia after pulmonary valve replacement [25], and the best predictor for left ventricular dysfunction [26]. The correlation between indexed right ventricular mass and indexed right ventricular wall thickness

was modest ($r = 0.27$–0.35) in this study, suggesting that measurement of right ventricular wall thickness seems to be insufficient for accurately evaluating right ventricular hypertrophy, and volumetric measurement of right ventricular mass is therefore crucial.

An iodinated contrast agent with a higher iodine concentration (400 mgI/mL) was used in this study to achieve higher cardiovascular enhancement, especially in the small vasculature such as the coronary artery and peripheral pulmonary vessels, at relatively lower injection rates (0.3–3.0 mL/s). As a result, a high iodine delivery rate (mgI/mL/sec), an important unit comprising both the iodine concentration and the injection rate for determining the degree of cardiovascular enhancement, can be obtained [19]. However, a lower iodine concentration contrast agent may be used in combination with the low tube voltage and iterative reconstruction technique in small patients without substantial compromise in cardiovascular enhancement and image noise [27,28].

This study has several limitations. First, no reference method was available to validate the right ventricular myocardial mass measurements. Nevertheless, closely correlated right ventricular mass values among the two different cardiac phases support the precision of the segmentation approach used in this study. Moreover, *ex vivo* validation of right ventricular mass measured using short-axis cine MRI and the threshold-based segmentation method was reported in excised human hearts after transplantation [29]. Second, the use of ionizing radiation in cardiac CT examination should be prudently justified for right ventricular mass quantification. In this study, the cardiac CT radiation dose was thoroughly optimized to minimize patient risks. For prospectively ECG-triggered sequential scan, the mean radiation dose was below 1.0 mSv. Furthermore, the mean radiation dose (6.1 mSv) of retrospectively ECG-gated spiral scan was comparable to that (6.2 mSv) reported using the prospectively ECG-triggered sequential scan [11]. The CT radiation dose level in this study might be relatively lower since it was for the whole thorax (a longer longitudinal scan range) in almost all cases, compared with previous studies where the whole heart (a shorter longitudinal scan range) was scanned by coronary CT angiography [11]. Third, this proposed method for right ventricular mass quantification should be tested by other investigators since this study was a single institution's experience.

In conclusion, CT quantification of right ventricular

mass using a semiautomatic 3D hybrid segmentation is technically applicable with high reproducibility in the majority of patients with cardiovascular disease.

Conflicts of Interest

The author has no potential conflicts of interest to disclose.

ORCID iD

Hyun Woo Goo

  https://orcid.org/0000-0001-6861-5958

REFERENCES

1. van Wolferen SA, Marcus JT, Boonstra A, Marques KM, Bronzwaer JG, Spreeuwenberg MD, et al. Prognostic value of right ventricular mass, volume, and function in idiopathic pulmonary arterial hypertension. *Eur Heart J* 2007;28:1250-1257

2. Hagger D, Condliffe R, Woodhouse N, Elliot CA, Armstrong IJ, Davies C, et al. Ventricular mass index correlates with pulmonary artery pressure and predicts survival in suspected systemic sclerosis-associated pulmonary arterial hypertension. *Rheumatology (Oxford)* 2009;48:1137-1142

3. Lu JC, Christensen JT, Yu S, Donohue JE, Ghadimi Mahani M, Agarwal PP, et al. Relation of right ventricular mass and volume to functional health status in repaired tetralogy of Fallot. *Am J Cardiol* 2014;114:1896-1901

4. Katz J, Whang J, Boxt LM, Barst RJ. Estimation of right ventricular mass in normal subjects and in patients with primary pulmonary hypertension by nuclear magnetic resonance imaging. *J Am Coll Cardiol* 1993;21:1475-1481

5. Bradlow WM, Hughes ML, Keenan NG, Bucciarelli-Ducci C, Assomull R, Gibbs JS, et al. Measuring the heart in pulmonary arterial hypertension (PAH): implications for trial study size. *J Magn Reson Imaging* 2010;31:117-124

6. Buechel EV, Kaiser T, Jackson C, Schmitz A, Kellenberger CJ. Normal right- and left ventricular volumes and myocardial mass in children measured by steady state free precession cardiovascular magnetic resonance. *J Cardiovasc Magn Reson* 2009;11:19

7. Freling HG, van Wijk K, Jaspers K, Pieper PG, Vermeulen KM, van Swieten JM, et al. Impact of right ventricular endocardial trabeculae on volumes and function assessed by CMR in patients with tetralogy of Fallot. *Int J Cardiovasc Imaging* 2013;29:625-631

8. van de Veerdonk MC, Dusoswa SA, Marcus JT, Bogaard HJ, Spruijt O, Kind T, et al. The importance of trabecular hypertrophy in right ventricular adaptation to chronic pressure overload. *Int J Cardiovasc Imaging* 2014;30:357-365

9. Koch K, Oellig F, Oberholzer K, Bender P, Kunz P, Mildenberger P, et al. Assessment of right ventricular function by 16-detector-row CT: comparison with magnetic resonance imaging. *Eur Radiol* 2005;15:312-318

10. Schwarz F, Takx R, Schoepf UJ, Lee YS, Ruzsics B, Gassner EM, et al. Reproducibility of left and right ventricular mass measurements with cardiac CT. *J Cardiovasc Comput Tomogr* 2011;5:317-324

11. Takx RA, Moscariello A, Schoepf UJ, Barraza JM Jr, Nance JW Jr, Bastarrika G, et al. Quantification of left and right ventricular function and myocardial mass: comparison of low-radiation dose 2nd generation dual-source CT and cardiac MRI. *Eur J Radiol* 2012;81:e598-e604

12. Rizvi A, Deaño RC, Bachman DP, Xiong G, Min JK, Truong QA. Analysis of ventricular function by CT. *J Cardiovasc Comput Tomogr* 2015;9:1-12

13. Goo HW. Technical feasibility of semiautomatic three-dimensional threshold-based cardiac computed tomography quantification of left ventricular mass. *Pediatr Radiol* 2019;49:318-326

14. Goo HW, Allmendinger T. Combined electrocardiography-and respiratory-triggered CT of the lung to reduce respiratory misregistration artifacts between imaging slabs in free-breathing children: initial experience. *Korean J Radiol* 2017;18:860-866

15. Goo HW. Combined prospectively electrocardiography- and respiratory-triggered sequential cardiac computed tomography in free-breathing children: success rate and image quality. *Pediatr Radiol* 2018;48:923-931

16. Goo HW. Comparison of chest pain protocols for electrocardiography-gated dual-source cardiothoracic CT in children and adults: the effect of tube current saturation on radiation dose reduction. *Korean J Radiol* 2018;19:23-31

17. Goo HW. Individualized volume CT dose index determined by cross-sectional area and mean density of the body to achieve uniform image noise of contrast-enhanced pediatric chest CT obtained at variable kV levels and with combined tube current modulation. *Pediatr Radiol* 2011;41:839-847

18. Goo HW. CT radiation dose optimization and estimation: an update for radiologists. *Korean J Radiol* 2012;13:1-11

19. Goo HW. State-of-the-art CT imaging techniques for congenital heart disease. *Korean J Radiol* 2010;11:4-18

20. Goo HW. Semiautomatic three-dimensional threshold-based cardiac computed tomography ventricular volumetry in repaired tetralogy of Fallot: comparison with cardiac magnetic resonance imaging. *Korean J Radiol* 2019;20:102-113

21. Goo HW, Park SJ, Yoo SJ. Advanced medical use of three-dimensional imaging in congenital heart disease: augmented reality, mixed reality, virtual reality, and three-dimensional printing. *Korean J Radiol* 2020;21:133-145

22. Winther HB, Hundt C, Schmidt B, Czerner C, Bauersachs J, Wacker F, et al. ν-net: deep learning for generalized biventricular mass and function parameters using multicenter cardiac MRI data. *JACC Cardiovasc Imaging* 2018;11:1036-1038

23. Robbers-Visser D, Boersma E, Helbing WA. Normal biventricular function, volumes, and mass in children aged 8

to 17 years. *J Magn Reson Imaging* 2009;29:552-559

24. Sarikouch S, Peters B, Gutberlet M, Leismann B, Kelter-Kloepping A, Koerperich H, et al. Sex-specific pediatric percentiles for ventricular size and mass as reference values for cardiac MRI: assessment by steady-state free-precession and phase-contrast MRI flow. *Circ Cardiovasc Imaging* 2010;3:65-76

25. Geva T, Mulder B, Gauvreau K, Babu-Narayan SV, Wald RM, Hickey K, et al. Preoperative predictors of death and sustained ventricular tachycardia after pulmonary valve replacement in patients with repaired tetralogy of Fallot enrolled in the INDICATOR cohort. *Circulation* 2018;138:2106-2115

26. Andrade AC, Jerosch-Herold M, Wegner P, Gabbert DD, Voges I, Pham M, et al. Determinants of left ventricular dysfunction and remodeling in patients with corrected tetralogy of Fallot. *J Am Heart Assoc* 2019;8:e009618

27. Andreini D, Mushtaq S, Conte E, Segurini C, Guglielmo M, Petullà M, et al. Coronary CT angiography with 80 kV tube voltage and low iodine concentration contrast agent in patients with low body weight. *J Cardiovasc Comput Tomogr* 2016;10:322-326

28. Wu Q, Wang Y, Kai H, Wang T, Tang X, Wang X, et al. Application of 80-kVp tube voltage, low-concentration contrast agent and iterative reconstruction in coronary CT angiography: evaluation of image quality and radiation dose. *Int J Clin Pract* 2016;70 Suppl 9B:B50-B55

29. Farber NJ, Reddy ST, Doyle M, Rayarao G, Thompson DV, Olson P, et al. Ex vivo cardiovascular magnetic resonance measurements of right and left ventricular mass compared with direct mass measurement in excised hearts after transplantation: a first human SSFP comparison. *J Cardiovasc Magn Reson* 2014;16:74